PROCEEDINGS A

royalsocietypublishing.org/journal/rspa

Research



Cite this article: Barkataki K, Panagiotou E. 2022 The Jones polynomial of collections of open curves in 3-space. *Proc. R. Soc. A* **478**: 20220302

https://doi.org/10.1098/rspa.2022.0302

Received: 5 May 2022 Accepted: 5 October 2022

Subject Areas:

topology, geometry, applied mathematics

Keywords:

open knots, links, knotoids, linkoids, Kauffman bracket polynomial, Jones polynomial

Author for correspondence:

Eleni Panagiotou

e-mail: Eleni.Panagiotou@asu.edu

The Jones polynomial of collections of open curves in 3-space

Kasturi Barkataki¹ and Eleni Panagiotou²

¹School of Mathematical and Statistical Sciences, Arizona State University, Tempe, AZ 85287-1804, USA
²Department of Mathematics and SimCenter, University of Tennessee at Chattanooga, 613 McCallie Avenue, Chattanooga, TN 37403, USA

KB, 0000-0003-3522-9270; EP, 0000-0002-1655-6447

Measuring the entanglement complexity of collections of open curves in 3-space has been an intractable, yet pressing mathematical problem, relevant to a plethora of physical systems, such as in polymers and biopolymers. In this manuscript, we give a novel definition of the Jones polynomial that generalizes the classic Jones polynomial to collections of open curves in 3-space. More precisely, first we provide a novel definition of the Jones polynomial of linkoids (open link diagrams) and show that this is a well-defined single variable polynomial that is a topological invariant, which, for link-type linkoids, coincides with that of the corresponding link. Using the framework introduced in (Panagiotou E, Kauffman L. 2020 Proc. R. Soc. A 476, 20200124. ((doi:10.1098/rspa.2020.0124)), this enables us to define the Jones polynomial of collections of open and closed curves in 3-space. For collections of open curves in 3-space, the Jones polynomial has real coefficients and it is a continuous function of the curves' coordinates. As the endpoints of the curves tend to coincide, the Jones polynomial tends to that of the resultant link. We demonstrate with numerical examples that the novel Jones polynomial enables us to characterize the topological/geometrical complexity of collections of open curves in 3-space for the first time.

1. Introduction

Many physical systems, such as polymers and biopolymers, textiles and chemical compounds are composed by filamentous structures, that can be modelled by mathematical curves in 3-space, whose entanglement complexity determines their mechanical properties and function [1–8]. Measuring multi-chain entanglement in such systems has remained an open problem for many decades [2,9,10]. In this paper, we introduce the first rigorous measure of complexity of collections of open curves in 3-space, via a traditional invariant of knots and links, the Jones polynomial. More precisely, the novel Jones polynomial that we introduce here generalizes the traditional Jones polynomial, so that it is applicable to collections of open curves in 3-space and gives a continuous measure of linking complexity which reduces to a topological invariant for closed curves.

Collections of simple closed curves in 3-space (links) can be classified upon deformations without allowing cutting and pasting (topological equivalence). Topological invariants are functions defined on links that are invariant under Reidemeister moves and can be used to characterize the complexity of simple closed curves in 3-space. The notion of topological equivalence, however, is not useful for systems of open curves in 3-space, since any collection of open curves is topologically equivalent to any other. Instead of topological invariants, to characterize the topological complexity of open curves in 3-space, we seek measures of topological complexity that are continuous functions in the space of configurations. Until recently, the only measure of topological entanglement that could be applied to one or two open curves in 3-space to give a continuous measure of single or pairwise topological complexity, was the Gauss linking integral [11-15]. It was not until [16], where the necessary framework to define the Jones polynomial of a single open curve in 3-space was introduced, based on the notion of knotoids (open ended knot diagrams) and their Jones polynomial. The Jones polynomial of an open curve is a polynomial with real coefficients that are continuous functions of the curve coordinates. This new framework also allowed to define Vassiliev measures of open curves in 3-space and to derive closed formulae for the second Vassiliev measure of single open curves in 3-space [17]. These advances led to immediate applications in materials and biology to obtain novel understanding of such physical systems, rigorously and without any closure scheme for the first time [18–20]. However, extending the Jones polynomial to collections of open curves in 3-space has not been possible, even though one would think it would be straightforward, as the definition of the classical Jones polynomial applies to both knots and links. The reason for this is that an appropriate definition of the Jones polynomial of linkoids (open ended link diagrams) is missing. This will be fully addressed in this manuscript.

The theory of knotoids was introduced by Turaev [21] as a means to study parts of knot diagrams with the aim to characterize knot complexity. Knotoids on a surface are open ended knot diagrams and many analogous ideas of classical knot theory are applicable to the study of knotoids [22–25]. The Jones polynomial of knotoids follows from that of knots with a simple modification. The modification relies on assigning a value to states containing an open arc in the bracket expansion. The notion of knotoids can be naturally extended to multi-component cases, which we call linkoids (these can be seen as open link diagrams). Even though the definition of the Jones polynomial of knots extends naturally to that of links, the definition of the Jones polynomial of linkoids does not follow directly from that of knotoids and remains elusive. The difficulty consists of the fact that the states resulting from linkoids may contain several nonintersecting open arcs, which may connect endpoints of different components, and it has been unclear how to deal with those in the polynomial. One way to deal with this is to introduce more variables to keep track of the connections [26]. Such definitions, however, do not satisfy an important property, which prevents them to be used in giving an appropriate definition of the Jones polynomial of open curves in 3-space, as we will see later. In this manuscript, we will provide a novel definition of the bracket polynomial that can properly account for those states and which satisfies an important desired property, which enables the definition of a single variable Jones polynomial of linkoids and the Jones polynomial of collections of open curves in 3-space.

More precisely, in this paper we provide the first rigorous definition of the Jones polynomial of linkoids which has the property that the Jones polynomial of a link-type linkoid is equal to the Jones polynomial of the corresponding link. We use the framework introduced in [16] to define

The contents of this paper are summarized as follows: in §2, we give the definitions for linkoid diagrams and linkoids and also make precise the notion of trivial linkoids, proper linkoids and link-type linkoids. In §3, we provide all the necessary framework and then define the Jones polynomial of linkoids and we study its properties. In §4, we give the definition of the Jones polynomial of a collection of open curves in 3-space and we study its properties. Finally, in §5, we present the conclusions of our results.

2. Linkoids

Downloaded from https://royalsocietypublishing.org/ on 06 January 2023

As mentioned in the previous section, the Jones polynomial of collections of open curves in 3-space will be defined via projections of the curves, which can be seen as linkoids. Even though we think of linkoids as projections of open curves, linkoids have been typically studied as diagrammatic objects. In this section, we present the definitions of linkoids and linkoid diagrams, originally defined in [22–25], as well as the definition of link-type linkoids. We denote a surface, which a linkoid diagram lies on, by the symbol Σ . In this manuscript, $\Sigma = S^2 = \mathbb{R}^2 \cup \infty$.

Definition 2.1. (Linkoid diagram) A linkoid diagram L with $n \in \mathbb{N}$ components in Σ is a generic immersion of $\bigsqcup_{i=1}^n [0,1]$ in the interior of Σ whose only singularities are transversal double points endowed with over/undercrossing data. These double points are called the crossings of L. The immersion of each [0,1] is referred to as a component of the linkoid diagram and the images of 0 and 1 under this immersion are called the foot and the head of the component, respectively. These two points are distinct from each other and from the double points; they are called the endpoints of the component. The diagram L has a total of 2n endpoints. A natural orientation is assigned for each l_i from the foot to the head.

For a linkoid diagram L with n components, we may introduce a convention to index all the feet by odd numbers $i \in \{1, 3, ..., 2n - 1\}$, and the corresponding heads by even numbers $i + 1 \in \{2, 4, ..., 2n\}$. Thus, a component of L is denoted by $l_{(2j-1,2j)}$ such that $j \in \{1, 2, ..., n\}$ where the index 2j - 1 indicates the foot and the index 2j indicates the head of the component.

Some examples of labelled knotoid and linkoid diagrams are given in figure 1.

Definition 2.2. (Linkoid) A linkoid is an equivalence class of linkoid diagrams up to the equivalence relation induced by the three Reidemeister moves and isotopy. The three Reidemeister moves, denoted by Ω_1 , Ω_2 , Ω_3 , are defined on linkoid diagrams and referred to as Ω -moves. It is forbidden to pull the strand adjacent to an endpoint over/under a transversal strand. These moves are called forbidden linkoid moves, and denoted by Φ_+ and Φ_- , respectively.

The Ω_1 , Ω_2 , Ω_3 moves and the forbidden linkoid moves, Φ_+ and Φ_- are shown in figure 2. In this manuscript, we consider the following definition of a trivial linkoid:

Definition 2.3. (Trivial linkoid) A trivial linkoid is one which consists of a collection of disjoint circles and/or straight segments. By disjoint we mean that there is no apparent crossing among the components of the linkoid.

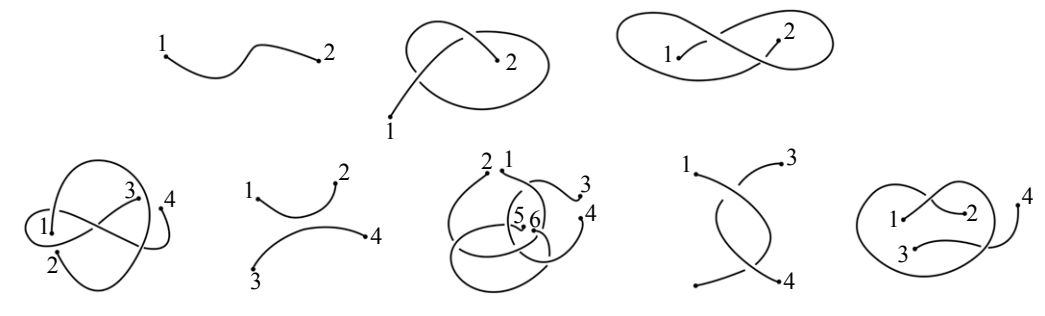


Figure 1. Examples of knotoid and linkoid diagrams with labelled components.

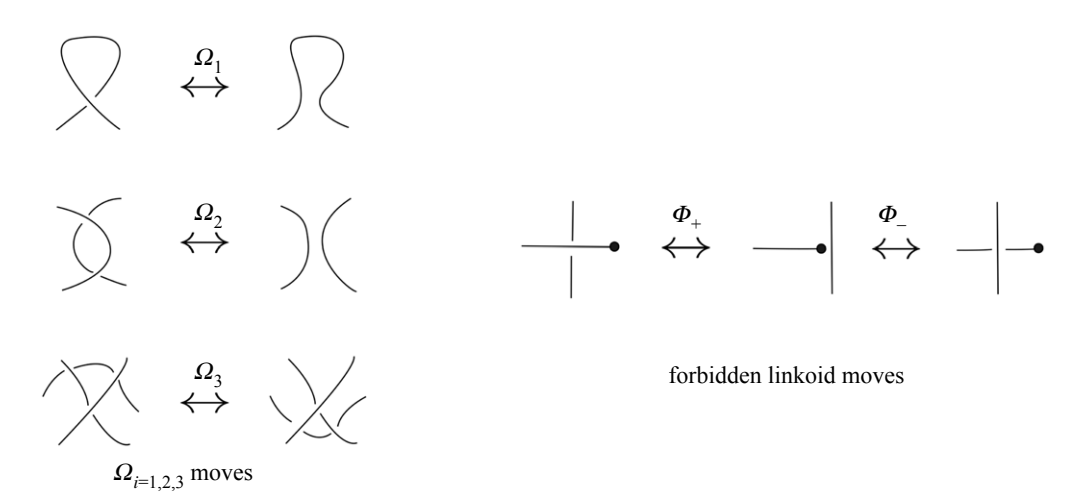


Figure 2. The Ω -moves and forbidden moves on a linkoid diagram. Note that these arcs are considered as parts of a larger diagram.

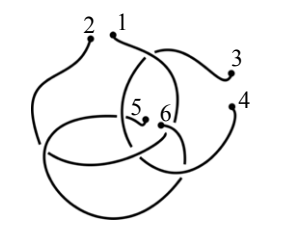


Figure 3. Examples of trivial linkoids consisting of two circles and two straight segments. Even though these are not equivalent, they will all be considered to represent the trivial linkoid with four components. Note that these are all link-type linkoids of the type of trivial links.

For a linkoid of one component, this definition coincides with that of a trivial knotoid. However, according to our definition of a trivial linkoid, definition 2.3, all the linkoids shown in figure 3 are equivalent, even though we cannot go from one diagram to the other without a forbidden linkoid move. Thus, when we refer to trivial linkoids, we refer to a collection of classes of linkoids with no crossings.

Definition 2.4. (Link-type linkoid and proper linkoid) A linkoid is said to be of link-type if there exists a diagram in its equivalence class in which it is possible to draw a closure arc connecting the pair of endpoints (from the head to the foot) per component without introducing additional double points (crossings) to the diagram or between the closure arcs. A linkoid that is not of link-type is called a proper linkoid.

Remark 2.5. The trivial linkoids shown in figure 3 are all of trivial link-type.



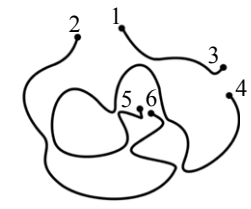


Figure 4. (Left) A linkoid diagram with three components, $I_{(1,2)}$, $I_{(3,4)}$ and $I_{(5,6)}$. (Right) One of the 64 possible states in the state sum expansion of the diagram. Clearly, this state is crossingless and contains three disjoint segments, namely (1, 3), (2, 6) and (4, 5). Note that even though the number of long segments is the same as the number of components of the original linkoid, there has been a rearrangement in the pairing of endpoints per segment.

Remark 2.6. For knotoids (linkoids with one component), another way to distinguish between proper knotoids and knot-type knotoids is by checking whether there exists a diagram in which the two endpoints lie in the same region. This definition is consistent with definition 2.4. Note that, if for any diagram of the knotoid it is impossible to draw a closure arc without introducing new crossings, it follows that the endpoints must lie in different regions of the diagram. The converse is also true.

Remark 2.7. Note that any pure braid (in a pure braid, the beginning and the end of each strand are in the same position) can be thought of as a link-type linkoid. Indeed, the closure arcs of a pure braid do not intersect any other arc, a trait similar to the closure arcs of a ink-type linkoid.

3. The Jones polynomial of linkoids

Downloaded from https://royalsocietypublishing.org/ on 06 January 2023

In this section, we will define the Jones polynomial of linkoids. As we mentioned in the introduction, this will be later seen as the Jones polynomial of a projection of a collection of open curves in 3-space. However, it is also of interest in the study of linkoids in general. We will define the Jones polynomial of linkoids as the normalized Kauffman bracket polynomial of linkoids.

The smoothing skein relations of the classic bracket polynomial are shown in equation (3.1), as follows:

$$\left\langle \sum \right\rangle = A \left\langle \sum \right\rangle + A^{-1} \left\langle \sum \right\rangle, \quad \left\langle L \cup \bigcirc \right\rangle = \left(-A^2 - A^{-2} \right) \left\langle L \right\rangle. \tag{3.1}$$

Definition 3.1. (State of a linkoid diagram) A state S of a linkoid diagram L with n components is an assignment of a choice of smoothing at each crossing. This results in a diagram without any apparent crossing with disjoint circles and n long segments. Each long segment is labelled by the two endpoints that it connects.

Upon recursively smoothing a linkoid diagram using the skein relations in equation (3.1), we obtain states without any apparent crossing. Figure 4 shows an illustrative example of a linkoid diagram with three components and one of its corresponding states.

Example 3.2. To motivate the relations that will enable us to evaluate the bracket polynomial on states involving multiple long segments, we focus on the particular example of the linkoid diagram shown in figure 5. Note that this linkoid diagram represents a link-type linkoid, corresponding to the Hopf link. It is natural to require that the bracket (and consequently the Jones) polynomial of the linkoid in this example reflects the entanglement present in the Hopf link. Note that the open Hopf-type linkoid is equivalent to a Hopf link with two $\epsilon > 0$ infinitesimal segments removed. Thus, it is natural to require that the bracket polynomial of the Hopf-type

linkoid is in fact equal to that of the Hopf link, which is equal to $\langle \bigcirc \rangle = -A^4 - A^{-4}$. This would in fact generalize the corresponding property of knot-type knotoids for the bracket (or Jones)

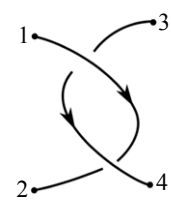


Figure 5. An oriented link-type linkoid with two components, corresponding to the Hopf link.

polynomial. In the following, it will be shown that this is also a necessary property to satisfy in order to define the Jones polynomial of open curves in 3-space in a way that it is well-behaved and satisfies some important properties.

Consider the oriented linkoid consisting of two components, as shown in figure 5. By smoothing the crossings in the linkoid diagram using the bracket polynomial definition for knotoids (see equation (3.1)), we get the following expansion:

$$\begin{pmatrix}
1 & 3 \\
2 & 4
\end{pmatrix} = A^{2} \begin{pmatrix}
1 & 3 \\
2 & 4
\end{pmatrix} + \begin{pmatrix}
1 & 3 \\
2 & 4
\end{pmatrix} + A^{-2} \begin{pmatrix}
1 & 3 \\
2 & 4
\end{pmatrix}$$

$$= A^{2} d \begin{pmatrix}
1 & 3 \\
2 & 4
\end{pmatrix} + 2 \begin{pmatrix}
1 & 3 \\
2 & 4
\end{pmatrix} + A^{-2} \begin{pmatrix}
1 & 3 \\
2 & 4
\end{pmatrix}$$

$$= (A^{2} d + 2) \begin{pmatrix}
1 & 3 \\
2 & 4
\end{pmatrix} + A^{-2} \begin{pmatrix}
1 & 3 \\
2 & 4
\end{pmatrix}, \tag{3.2}$$

where $d = -A^2 - A^{-2}$.

The final expression in equation (3.2) is a summation of bracket polynomials of states of the linkoid diagram with two long segments each. Note that the Kauffman bracket polynomial of knotoids can evaluate the bracket of an open arc, simply by setting $\langle \bullet \rangle = 1$, but in linkoids we will have more than one long arc in a state, as shown in equation (3.2). Moreover, even though each of the states consist of two long segments, the segments connect different endpoints of the original components, as shown in equation (3.2). For this reason, even though the Jones polynomial of links only accounts for the number of components in a state, this will not work for linkoids. For example, if we assign the same value to both of the cases in equation (3.2), say

$$\left\langle \begin{array}{c} \begin{array}{c} \\ \\ \end{array} \right\rangle = \left\langle \begin{array}{c} \\ \end{array} \right\rangle \left\langle \begin{array}{c} \\ \end{array} \right\rangle = t$$
, then $\left\langle \begin{array}{c} \\ \end{array} \right\rangle = \left(A^2d + 2 + A^{-2}\right)t = \left(-A^4 + A^{-2} + 1\right)t$, which is different from the bracket polynomial of the Hopf link, even if we set $t = d$.

In this manuscript, we introduce a new definition of the Jones polynomial of linkoids that overcomes these problems. The section is organized as follows: §3a sets the framework for analysing states of linkoids, §3b gives the novel Jones and Kauffman bracket polynomial definitions and §3c proves theorem 3.12.

(a) Segment cycles of a linkoid state

The definition of the Jones polynomial that is introduced in §3b relies on assigning a value to the trivial states that result after smoothing all the crossings in a linkoid diagram. Circles in a state will contribute a factor $d^{|\text{circ}|-1}$, where |circ| is the number of disjoint circles in the state, but arcs will contribute a factor $d^{|\text{cyc}|}$, where |cyc| is the number of segment cycles in the state. A segment cycle is composed by the arcs of a state that form a component upon concatenation of their endpoints according to the original head/foot pairing. See figure 7 for two states that correspond to one and two segment cycles, respectively. This section focuses on the detailed mathematical framework leading to the definition of segment cycles and some of their properties.

Let L be a linkoid diagram with $n \in \mathbb{N}$ components and let G be the set containing all the endpoints (heads and feet) of L. In a smoothed state of L, the pairwise connections between vertices in G may turn out to be different from the original (2j-1,2j) pairing, where $j \in \{1,2,\ldots,n\}$. To keep track of how the different vertices get permuted in a state, we introduce the definition for pairing combination.

Definition 3.3. (Pairing combination and head–foot pairing) Let S_{2n} denote the symmetry group of degree 2n, where $n \in \mathbb{N}$. A pairing combination is any element $J \in S_{2n}$ which can be expressed as the product of n disjoint two-cycles. In particular, the element,

$$\Gamma = (1 \quad 2)(3 \quad 4) \cdots (2n-1 \quad 2n) = \prod_{i=1}^{n} (2i-1 \quad 2i),$$
 (3.3)

is defined to be the head–foot pairing in S_{2n} . In this notation, a bracketed sequence of numbers signifies a permutation in S_{2n} which are also called two-cycles.

Note that any linkoid defines a head–foot pairing (see definition 2.1) by the connectivity of its components. Whereas, a state of a linkoid diagram, S, defines a pairing combination, J_S , which may or may not be a head–foot pairing.

For any endpoint, we introduce the concept of orbit to form a collection of all the other endpoints that it is related to under a repeated application of the composition function $\Gamma \circ J$. This captures all the arc endpoints connected to a given endpoint, either through the initial head–foot pairing, or through smoothings of crossings.

Definition 3.4. (Orbit of an endpoint) Given an endpoint $a \in G$, and an arbitrary pairing combination, J on G, the set $\operatorname{Orb}_{J}(a)$ of a is defined to be the orbit of the composition function $\Gamma \circ J$. Symbolically, $\operatorname{Orb}_{J}(a)$ is given as

$$Orb_{I}(a) = \{ x \in G | x = (\Gamma \circ I)^{m}(a), \quad m \in \mathbb{Z} \}.$$

$$(3.4)$$

This enables us to define the segment cycle in terms of pairing combinations and orbits, as follows:

Downloaded from https://royalsocietypublishing.org/ on 06 January 2023

Definition 3.5. (Segment cycle) Given a pairing combination, J on G, the segment cycle of an endpoint $a \in G$ is defined as follows:

$$Seg(a) = Orb_{J}(a) \bigcup Orb_{J}(\Gamma(a)), \tag{3.5}$$

where $\operatorname{Orb}_J(a)$ is the orbit of the point a and $\operatorname{Orb}_J(\Gamma(a))$ is the orbit of the point $\Gamma(a)$ under the action of the pairing combination J. Note that for any point $a \in G$, $\Gamma(a) \in G$ always belongs to the same segment cycle. Thus, a segment cycle always contains an even number of elements.

Remark 3.6. Let S denote a state of L with associated pairing J_S , and let Seg(a) be a segment cycle in L, such that |Seg(a)| = 2k. Then, we can represent Seg(a) by a circle decorated with the 2k endpoints of L (see figure 6), following the order in which they appear in the cycle (see figure 6). Note that the arcs connecting two adjacent points in this circle alternate between the functions, J_S and Γ . Any two points connected by J_S belong to the same component of the state S and any two points connected by Γ belong to the same component in L.

Example 1 (cont.) Consider the linkoid diagram and the particular state (say S) as shown in figure 5. In this example, the set G of all endpoints is $\{1, 2, 3, 4\}$. Note that the open arc components of a linkoid diagram L define a head–foot pairing, while the states of L can define other pairing combinations. For example, let us denote by s_1, s_2 the final states of equation (3.2). Then, s_1 defines the pairing combination J_{s_1} , which can be represented by the permutation (1 3)(2 4) $\in S_4$ and s_2 defines the pairing combination J_{s_2} , which can be represented by the permutation (1 2)(3 4) $\in S_4$. The states s_1 and s_2 are explicitly shown in figure 7.

For each of the permutations, J_{s_1} and J_{s_2} , we can construct the corresponding set of segment cycles. Note that a segment cycle can be represented as a decorated circle. Corresponding to J_{s_1} and J_{s_2} , the possible segment cycles are shown in figure 7.

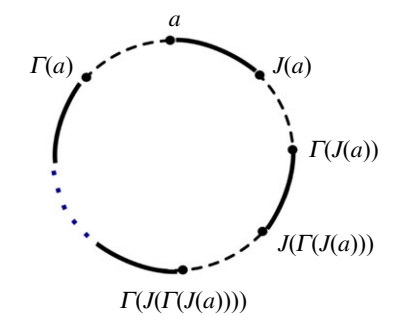


Figure 6. Representation of the segment cycle of $a \in G$ in terms of a decorated circle. Let us consider a circle and let $a \in G$ be the initial point on the circle. The remaining 2k-1 endpoints can be uniquely added into the circle in the order J(a), $\Gamma(J(a))$, $J(\Gamma(J(a)))$, . . . , up to $\Gamma(a)$. Note that the arcs connecting two adjacent points in this circle alternate between the functions, J (solid) and Γ (dashed). Any two points connected by J belong to the same component of the state S and any two points connected by Γ belong to the same component in S. (The dotted line in the figure indicates the continued process of adding points.)

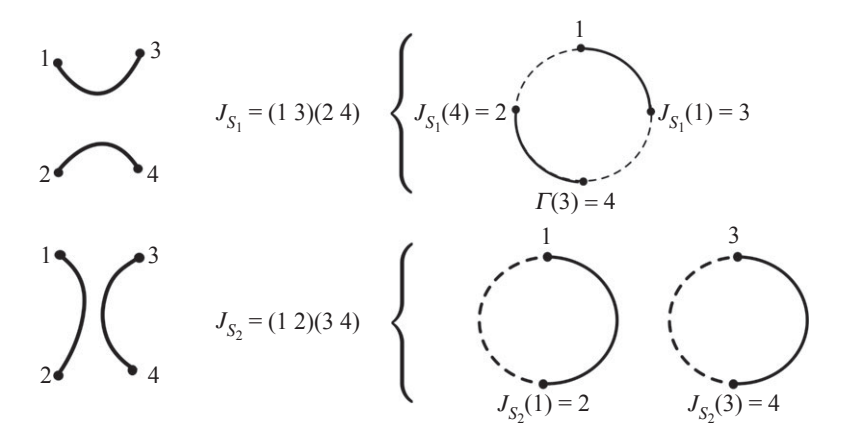


Figure 7. (Top) The connections among endpoints due to state s_1 , corresponding to the pairing combination $J_{s_1} = (1 \quad 3)(2 \quad 4) \in S_4$, and the resultant segment cycle. (Bottom) The connections among endpoints due to state s_2 , corresponding to the pairing combination $J_{s_2} = (1 \quad 2)(3 \quad 4) \in S_4$, and the resultant distinct segment cycles.

Remark 3.7. Note that for a linkoid with n components, the total number of distinct segment cycles in a state always lies between 1 and n. Indeed, if the resulting long arcs are the same as the original arcs, then each one defines a segment cycle. On the other hand, if all the long arcs have been relabelled so that we can concatenate them all together, according to their original head/foot pairings, then they will form one segment cycle. A formal proof of this result is given in proposition A.9 in appendix A.

(b) The Jones polynomial of linkoids

In the previous section, we showed that open segments in a smoothed state of a linkoid can be grouped into segment cycles. We also saw the analogy between segment cycles and decorated circles. In this section, we use these concepts to define the bracket polynomial of linkoids and the Jones polynomial of linkoids (as the normalized bracket polynomial).

Definition 3.8. (Bracket polynomial of a linkoid) Let L be a linkoid diagram with n components. The bracket polynomial of the linkoid is completely characterized by the following skein relation

and initial conditions:

$$\left\langle \begin{array}{c} \left\langle \right\rangle \right\rangle = A \left\langle \begin{array}{c} \left\langle \right\rangle \right\rangle + A^{-1} \left\langle \right\rangle \left\langle \right\rangle, \quad \left\langle L \cup \bigcirc \right\rangle = \left(-A^2 - A^{-2} \right) \left\langle L \right\rangle, \\ \left\langle \left\langle \right\rangle \right\rangle = \left(-A^2 - A^{-2} \right)^{|cyc|}. \tag{3.6}$$

where |cyc| denotes the number of distinct segment cycles. In other words, $|\text{cyc}| = |G/\mathcal{R}_{\mathcal{G}}|$, where $\mathcal{R}_{\mathcal{G}}$ is the equivalence relation induced on G by $\mathcal{G} = \langle \Gamma \circ J \rangle \times \langle \Gamma \rangle$, where J is the pairing defined by the indices $a, b, c, d, \dots p, q$.

The bracket polynomial of *L* can be formulated as the following state sum expression:

$$\langle L \rangle := \sum_{S} A^{\sigma(S)} d^{|S|_{\text{circ}} + |S|_{\text{cyc}} - 1}, \tag{3.7}$$

where S is a state corresponding to a choice of smoothing over all double points in L; $\sigma(S)$ is the algebraic sum of the smoothing labels of S; $|S|_{circ}$ is the number of disjoint circles in S and $|S|_{cyc}$ is the number of distinct segment cycles in S.

The bracket polynomial of linkoids has the following properties:

- It preserves the underlying skein relation used in the computation of bracket polynomial of knots and knotoids.
- (ii) If L is a link diagram, the novel definition of the bracket polynomial (see definition 3.8) coincides with the traditional Kauffman bracket polynomial of L. Indeed, the states of L have no long segments. Therefore, $|S|_{\text{cyc}} = 0$ and

$$\langle L \rangle = \sum_{S} A^{\sigma(S)} d^{|S|_{\text{circ}} - 1}.$$

(iii) If L is a knotoid diagram, then the novel definition of the bracket polynomial (see definition 3.8) coincides with the Kauffman bracket polynomial of knotoids. Indeed, for a knotoid, $|S|_{cyc} = 1$ for all states and

$$\langle L \rangle = \sum_{S} A^{\sigma(S)} d^{|S|_{\text{circ}} - 1} d^1 = \sum_{S} A^{\sigma(S)} d^{|S|_{\text{circ}}}.$$

(iv) For a trivial linkoid (see definition 2.3) with *n* components,

$$\langle L \rangle = d^{n-1}.$$

Indeed, for a trivial linkoid with *n* components, there are no rearrangements in the pairing of endpoints since there are no crossings to be resolved. Therefore, there is only one state in the state sum which has the original *n* segments and their endpoints intact and

$$\langle L \rangle = A^0 \times d^{0-1} \times d^n = d^{n-1}.$$

(vi) For link-type linkoids the bracket polynomial coincides with that of the corresponding link upon the closure of endpoints (see theorem 3.12).

In the following, the bracket polynomial turns into an invariant for oriented linkoids with a normalization by the writhe giving rise to a definition for the Jones polynomial of linkoids with the substitution of $A = t^{-1/4}$. The writhe, Wr(L), of an oriented linkoid diagram L is the algebraic sum of signs (positive or negative) of crossings of L.

Figure 8. Two non-equivalent, proper linkoids. Their Jones polynomials in terms of the variable A are (a) $-A^4 - A^2$ and (b) $-A^{-2} - A^{-4}$.

Definition 3.9. (Jones polynomial of a linkoid) The normalized bracket polynomial of an oriented linkoid diagram L is defined as

$$f_L = (-A^3)^{-Wr(L)} \langle L \rangle, \tag{3.8}$$

where Wr(L) is the writhe of the linkoid diagram and $\langle L \rangle$ is as seen in definition 3.8. This gives the Jones polynomial of a linkoid with the substitution $A = t^{-1/4}$.

Example 3.10. The Jones polynomial (definition 3.9) distinguishes non-equivalent linkoids in S^2 and for proper linkoids, this measure is not that of any link. For example the Jones polynomial of the linkoid given in figure 8a is equal to $\int_{-\infty}^{6a} (1-A^4 - A^2) dt$ whereas, the Jones polynomial of the linkoid given in figure 8b is equal to $\int_{-\infty}^{6a} (1-A^4 - A^2) dt$

Proposition 3.11. The Jones polynomial of a linkoid (see definition 3.9) is a topological invariant of linkoids.

Proof. The above claim is proved by verifying invariance of the Jones polynomial of linkoids under each of the three Reidemeister moves, which are discussed as follows:

Downloaded from https://royalsocietypublishing.org/ on 06 January 2023

Reidemeister move I: in a linkoid diagram, L, consider a region that resembles \bigcirc . Let M denote the same linkoid except at that particular region, which now resembles \bigcirc . The Jones polynomial of L is equal to the Jones polynomial of M, as shown below:

$$f_{L} = \left(-A^{3}\right)^{-Wr(L)} \left\langle \bigcirc \right\rangle$$

$$= \left(-A^{3}\right)^{-Wr(L)} \left[A\left\langle \bigcirc \right\rangle + A^{-1}\left\langle \bigcirc \right\rangle \right]$$

$$= \left(-A^{3}\right)^{-Wr(L)} \left[A\left\langle \bigcirc \right\rangle + A^{-1}\left(-A^{2} - A^{-2}\right)\left\langle \bigcirc \right\rangle \right]$$

$$= \left(-A^{3}\right)^{-Wr(L)} \left(-A^{-3}\right) \left\langle \bigcirc \right\rangle$$

$$= \left(-A^{3}\right)^{-Wr(L)} \left(-A^{-3}\right) \left\langle \bigcirc \right\rangle$$

$$= \left(-A^{3}\right)^{-Wr(L)-1} \left\langle \bigcirc \right\rangle$$

$$= f_{M}. \tag{3.9}$$

Reidemeister move II: in a linkoid diagram, L, consider a region that resembles \bigcirc . Let M denote the same linkoid except at that particular region, which now resembles \bigcirc . Note that Wr(L) = Wr(M), since the regions \bigcirc and \bigcirc contribute zero writhe, respectively. The Jones

polynomial of *L* is equal to the Jones polynomial of *M*, as shown below:

$$f_{L} = \left(-A^{3}\right)^{-Wr(L)} \left\langle \bigcirc \right\rangle$$

$$= \left(-A^{3}\right)^{-Wr(L)} \left[A^{-2}\left\langle \bigcirc \right\rangle + A^{2}\left\langle \bigcirc \right\rangle + \left\langle \bigcirc \right\rangle + \left\langle \bigcirc \right\rangle\right)$$

$$= \left(-A^{3}\right)^{-Wr(L)} \left[\left(A^{2} + A^{-2}\right)\left\langle \bigcirc \right\rangle + \left\langle \bigcirc \right\rangle + \left(-A^{2} - A^{-2}\right)\left\langle \bigcirc \right\rangle\right]$$

$$= \left(-A^{3}\right)^{-Wr(M)} \left\langle \bigcirc \right\rangle$$

$$= f_{M}. \tag{3.10}$$

Reidemeister move III: since the traditional bracket polynomial skein relations are preserved in our new Jones polynomial definition, the proof of invariance under Reidemeister move III follows in a way similar to the above two cases.

The Jones polynomial of linkoids (see definition 3.9) has the following properties:

(i) The Jones polynomial of a linkoid is a topological invariant of linkoids and it satisfies the Jones polynomial skein relations:

$$t^{-1}f_{L_{+}} - tf_{L_{-}} = (t^{1/2} - t^{-1/2})f_{L_{0}},$$

where the linkoids L_+ , L_- and L_0 are identical almost everywhere except at one crossing, as shown below:



(ii) If L is a link diagram, then the new definition of the Jones polynomial (see definition 3.9) gives the traditional Jones polynomial of the link. Indeed, for a link L, there is no long segment. Therefore, $|S|_{\text{cyc}} = 0$ and

$$f_L = (-A^3)^{-Wr(L)} \sum_S A^{\sigma(S)} d^{|S|_{\text{circ}} - 1} d^0.$$

(iii) If L is a knotoid diagram, the Jones polynomial of L (see definition 3.9) coincides with the Jones polynomial of knotoids. Indeed, if L has only one component, then $|S|_{\rm cyc} = 1$ (only one long segment) for all states and

$$f_L = (-A^3)^{-Wr(L)} \sum_{S} A^{\sigma(S)} d^{|S|_{\text{circ}}}.$$

(iv) For a trivial linkoid (see definition 2.3) with *n* components,

Downloaded from https://royalsocietypublishing.org/ on 06 January 2023

$$f_L = d^{n-1}$$
.

Indeed, in that case there are no rearrangements in the pairing of endpoints since there are no crossings to be resolved. Therefore, there is only one state in the state sum which has the original n segments and their endpoints intact. Since there are no crossings, the writhe is zero and this allows us to express the Jones polynomial as

$$f_L = (-A^3)^0 A^0 \times d^{0-1} \times d^n = d^{n-1}$$

(v) For link-type linkoids the Jones polynomial coincides with that of the corresponding link (see theorem 3.12).

Example 3.2 (cont.) Let us return to the example of a linkoid diagram with two components, as given in figure 5. Here, the set G of endpoints is equal to $\{1, 2, 3, 4\}$. The final step of the state

royalsocietypublishing.org/journal/rspa Proc. R. Soc. A 478: 20220302

of the two states 2 and 2 \sqrt{4} and 2 \sqrt{5}. These give rise to the segment cycles shown in figure 7. More precisely, let us call the states by s_1 and s_2 , respectively, and their respective pairing combinations as J_{s_1} and J_{s_2} . Note that $J_{s_2} = \Gamma = (1 \ 2)(3 \ 4)$ implies that there are two distinct segment cycles corresponding to s_2 , namely $Seg(1) = \{1, 2\}$ and $Seg(3) = \{3, 4\}$. Whereas, the action of $J_{S_1} = (1 \quad 3)(2 \quad 4)$ on G gives $Seg(1) = \{1, 2, 3, 4\} = G$. Therefore, there is only one distinct segment cycle corresponding to s_1 .

sum expansion of its bracket polynomial (see equation (3.2)) involves the bracket polynomials

Using definition 3.8, the final step of equation (3.2) can be simplified as follows:

$$\begin{pmatrix}
1 & 3 \\
2 & 4
\end{pmatrix} = (A^2d + 2) \begin{pmatrix}
1 & 3 \\
2 & 4
\end{pmatrix} + A^{-2} \begin{pmatrix}
1 & 3 \\
2 & 4
\end{pmatrix}$$

$$= (A^2d + 2)d^{0-1}d^1 + A^{-2}d^{0-1}d^2$$

$$= -A^4 - A^{-4}.$$
(3.11)

Note that the above expression matches the bracket polynomial for the Hopf link, i.e. $\left\langle \left(\bigcap\right)\right\rangle = -A^4 - A^{-4}$. The writhe of the diagram in figure 5 is (5) . Therefore, the Jones polynomial of the linkoid is evaluated as follows:

$$f_{N} = (-A^{3})^{-Wr(N)} \left\langle \sum_{2}^{1} \sum_{4}^{3} \right\rangle$$
$$= (-A^{3})^{2} (-A^{4} - A^{-4})$$
$$= -A^{10} - A^{2}, \tag{3.12}$$

which is equal to that of the Hopf link. In fact, we will prove that a similar result follows for the case for any link-type linkoid.

(c) The Jones polynomial of link-type linkoids

In this section, we will prove that the Jones polynomial of link-type linkoids is equal to the Jones polynomial of the corresponding link.

Theorem 3.12. Let L be a link-type linkoid with n components and L_c be the corresponding link (the link that results from connecting the head to the foot of each component in a way that no new crossing is *created*). Then, the Jones polynomials of L and L_c are equal, that is $f_L = f_{L_c}$.

Proof. By the definition of L and L_c , we note that L can be created from L_c by omitting n arcs (closure arcs). These arcs connect the endpoints 2j-1 and 2j for each component $l_{(2j-1,2j)}$ of L, where $j \in G = \{1, 2, ..., n\}$. Let us construct a decoration on L_c by L, by keeping track of the endpoints of L with labels. Thus L_c is a union of L with closure arcs.

The closure arcs in L do not create any new crossings, hence the total number of double points in L_c is the same as that in L. Therefore, $Wr(L) = Wr(L_c)$. In the following, we show that the bracket polynomials, $\langle L \rangle$ and $\langle L_c \rangle$, are also equal.

We know that the states of a link or a linkoid diagram are completely determined by the choice of smoothing at the crossings of the diagram. Since L and L_c have identical crossings, for each state S of the linkoid diagram L, there exists a state S_c in the link diagram L_c , such that their smoothing labels are equal, that is, $\sigma(S) = \sigma(S_c)$. By definition, the contribution of S in the state sum expression of $\langle L \rangle$ is $A^{\sigma(S)}d^{|S|_{circ}+|S|_{cyc}-1}$, where $|S|_{circ}$ is the number of disjoint circles and $|S|_{cyc}$ is the number of segment cycles formed by the disjoint long segments in the state S. Similarly, the contribution of S_c in the state sum expression of $\langle L_c \rangle$ is $A^{\sigma(S)}d^{|S_c|_{circ}-1}$. We prove that these two terms are equal by showing that $|S|_{circ} + |S|_{cyc} = |S_c|_{circ}$.

Since the closure arcs of L in L_c do not introduce crossings, the state S can be obtained from S_c , by omitting the closure arcs. Thus, for a decorated L_c , S_c will also be decorated with an even number of labels on each circle (since any closure arc has two endpoints and closure arcs are disjoint). Note that if a circle in S_c is not decorated, then it corresponds to a circle in S. Let us express the total number of circles in S_c as $|S_c|_{\text{circ}} = |S_c|_{(\text{circ},u)} + |S_c|_{(\text{circ},d)}$, where $|S_c|_{(\text{circ},u)}$ and $|S_c|_{(\text{circ},d)}$ denote the number of undecorated and decorated circles, respectively. Thus, $|S|_{\text{circ}} = |S_c|_{(\text{circ},u)}$. Therefore, we need to prove that $|S|_{\text{cyc}} = |S_c|_{(\text{circ},d)}$.

Once all the circles that do not involve endpoints are taken care of in both S and S_c , we are left with n long segments in S and a total of $|S_c|_{(\text{circ},d)}$ decorated circles in S_c . Since S is formed by S_c by removing the closure arcs, a decorated circle in S_c with 2k labels gives rise to k long segments in S. We show that these k long segments form a segment cycle.

Note that for a decorated circle in S_c , two adjacent labels are either endpoints of a closure arc, or a new connection formed by the smoothings. So, any two adjacent labels in a decorated circle in S_c that do not belong to a closure arc are related by the pairing combination J_S in S and any two adjacent labels in the decorated circle in S_c that belong to the same closure arc are related by the trivial pairing, Γ . Then, the corresponding k long segments in S define a segment cycle. These k long segments cannot overlap with any other decorated circle of S_c because it will violate the fact that all the decorated circles of S_c are disjoint. Therefore, for every decorated circle in S_c there is a unique collection of long segments in S such that these long segments form a segment cycle. This implies, $|S_c|_{\text{(circ,d)}} = |S|_{\text{cyc}}$. Therefore, $\langle L \rangle = \langle L_c \rangle$.

4. The Jones polynomial of open curves in 3-space

Consider a collection of $m \in \mathbb{N}$ open or closed curves in 3-space in general position. Any (regular) projection of these curves can give rise to a different linkoid diagram based on the choice of the direction of projection. Note that with probability one, a projection will be generic. We use the framework introduced in [16] and definition 3.8, to rigorously define the bracket and Jones polynomials of a collection of $m \in \mathbb{N}$ open curves in 3-space. We define the Jones polynomial as the normalized bracket polynomial.

Definition 4.1. Let \mathcal{L} denote a collection of $m \in \mathbb{N}$ open curves in 3-space. Let \mathcal{L}_{ξ} denote the projection of \mathcal{L} on a plane with normal vector ξ . The normalized bracket polynomial of \mathcal{L} is defined as

$$f_{\mathcal{L}} = \frac{1}{4\pi} \int_{\xi \in S^2} (-A^3)^{-Wr(\mathcal{L}_{\xi})} \langle \mathcal{L}_{\xi} \rangle dS.$$
 (4.1)

where each \mathcal{L}_{ξ} is a linkoid diagram and its bracket polynomial can be calculated by using definition 3.8. Note that the integral is taken over all vectors $\xi \in S^2$ except a set of measure zero (corresponding to the irregular projections). This gives the Jones polynomial of a collection of open curves in 3-space with the substitution $A = t^{-1/4}$.

This new definition of the Jones polynomial of collections of open or closed curves in 3-space generalizes all the previous definitions of the Jones polynomial, so that it satisfies the following properties:

- (i) The Jones polynomial defined by equation (4.1) does not depend on any particular projection of the collection of open or closed curves.
- (ii) For a collection of open curves this polynomial is not the polynomial of a corresponding/approximating link, nor that of a corresponding/approximating linkoid.
- (iii) The Jones polynomial of a collection of open curves in 3-space has real coefficients. It is not a topological invariant, but it is a continuous function of the curve coordinates (see proposition 4.2).
- (iv) For a collection of closed curves in 3-space (a link), the Jones polynomial defined in equation (4.1) gives the traditional Jones polynomial and it can be computed from a single projection, i.e. $f_{\mathcal{L}} = f_{\mathcal{L}_{\xi}}$ where $\xi \in S^2$ is any projection vector.

the Jones polynomial defined in [16].

Downloaded from https://royalsocietypublishing.org/ on 06 January 2023

In the case of polygonal curves in 3-space, the Jones polynomial attains a simpler expression. Without loss of generality, suppose that all the curves have n edges each. Then, there exists a finite number (say $k \in \mathbb{N}$) of distinct linkoid types (L_i) which may occur in any projection of the collection of open curves, \mathcal{L} . Therefore, equation (4.5) can also be expressed as the following finite sum:

$$f_{\mathcal{L}} = \sum_{i=1}^{k} p_{i} f_{L_{i}},\tag{4.2}$$

where p_i denotes the geometric probability that a projection of \mathcal{L} gives the linkoid L_i .

Proposition 4.2. Let \mathcal{L} denote a collection of simple open curves in 3-space. Then, $f_{\mathcal{L}}$ is a continuous function of the coordinates of \mathcal{L} .

Proof. Let us approximate \mathcal{L} by a set of polygonal curves of n edges each, we denote $\mathcal{L}^{(n)}$. Then

$$f_{\mathcal{L}^{(n)}} = \sum_{i=1}^{k} p_{i} f_{L_{i}^{(n)}}, \tag{4.3}$$

where $L_i^{(n)}$, i = 1, ..., k are the possible linkoids that can occur in all projections of $\mathcal{L}^{(n)}$ and p_i the corresponding geometric probabilities. The geometric probability p_i can be expressed as

$$p_i = \frac{2A_0}{4\pi},\tag{4.4}$$

where A_0 is the area on the sphere corresponding to vectors $\boldsymbol{\xi} \in S^2$ such that the projection of $\mathcal{L}^{(n)}$ along such vectors results in the linkoid $L_i^{(n)}$. A_0 is a quadrangle bounded by great circles defined by the edges and vertices of the polygonal curves in $\mathcal{L}^{(n)}$. Thus it is a continuous function of the coordinates of $L^{(n)}$ (see proof of lemma 3.1 in [16]). The result follows as n goes to infinity.

Corollary 4.3. Let L denote a collection of open curves in 3-space. As the endpoints of the curves tend to coincide to form a link L_c , f_L tends to f_{L_c}

Proof. The result follows by proposition 4.2, definition 4.1 and theorem 3.12.

The statement below follows as a corollary from the properties of the Jones polynomial of open and closed curves in 3-space that we have established so far.

Corollary 4.4. The Jones polynomial is a continuous function in the space of all simple curves (open or closed) in 3-space.

In a similar way, we can define the Kauffman bracket polynomial of a collection of open curves in 3-space, as follows:

Definition 4.5. Let \mathcal{L} denote a collection of $n \in \mathbb{N}$ open curves in 3-space. Let \mathcal{L}_{ξ} denote the projection of \mathcal{L} on a plane with normal vector ξ . The bracket polynomial of \mathcal{L} is defined as

$$\langle \mathcal{L} \rangle = \frac{1}{4\pi} \int_{\xi \in S^2} \langle \mathcal{L}_{\xi} \rangle \, \mathrm{d}S,$$
 (4.5)

where each \mathcal{L}_{ξ} is a linkoid diagram and its bracket polynomial can be calculated by using definition 3.8. Note that the integral is taken over all vectors $\xi \in S^2$ except a set of measure zero (corresponding to the irregular projections).

royalsocietypublishing.org/journal/rspa Proc. R. Soc. A 478: 20220302

Properties of the bracket polynomial of collections of open curves in 3-space:

- (i) The bracket polynomial defined in equation (4.5) does not depend on any particular projection of the collection of curves.
- (ii) For an open curve this polynomial is not the polynomial of a corresponding/approximating link, nor that of a corresponding/approximating linkoid.
- (iii) The bracket polynomial defined in equation (4.5) is not a topological invariant, but it is a continuous function of the curve coordinates for both open and closed curves in 3-space.
- (iv) As the endpoints of a collection of open curves in 3-space tend to coincide, the bracket polynomial tends to that of the corresponding link.
- (v) For a linkoid of one component, the bracket polynomial of definition 4.5 gives the bracket polynomial defined in [16].

Example 4.6. Consider a set of open borromean rings realized in 3-space by the following three lists of coordinates:

```
R = [[0, 0, 0], [1, 1, 0], [2, 2, 0.5], [3, 3, 0.5],
   [4, 4, 0], [5, 5, 0], [6, 6, 0.5], [7, 7, 0.5],
   [8, 7, 0.5], [9, 5, 0.2], [9, 3, 0.2], [8, 0, 0.2], [8, -1, 0.2],
   [6, -1.5, 0], [4, -2, 0], [2, -1.5, 0]]
B = [[1, 0, 0.5], [4, 0, 0], [5, 1, 0], [5, 4, 0.5], [4, 5, 0.5],
   [3, 6, 0], [2, 7, 0], [-1, 6, 0], [-1, 3, 0.5]]
K = [[6, 0, 0.5], [7, 6, 0], [6, 7, 0], [3, 7, 0.5], [2, 6, 0.5],
   [2, 3, 0], [3, 2, 0], [4, 1, 0.5]]
```

where R, B and K denote the red, blue and black curves, respectively. The list R can be updated by an additional element (say r) by using the following parametrization:

$$r = r_1 + s(r_2 - r_1),$$

where $0 \le s \le 1$ and r_1 and r_2 are, respectively, the last and the first points in R, i.e. $r_1 = \mathbb{R}[-1]$ and $r_2 = \mathbb{R}[0]$. Using the same parameter s, the lists B and K can each be updated by an additional element.

Let us denote a configuration of the system of open borromean rings by w(s), where s is the value of the concerned parameter. Clearly, the initial configuration of the system of open borromean rings can thus be denoted as w(0). As we start updating the lists R, B and K by the above parametrization, the endpoints of each component of w(0) move closer and closer in time, eventually attaining the configuration of the closed borromean rings, namely w(1). The coefficients of the Jones polynomial change with the deformation and are continuous functions of the chain coordinates. The Jones polyomials of the collection of curves from the initial to the final stage, along with some intermediate steps, are presented in figure 9 and their explicit expressions are given as follows:

$$f_{w(0)} = -0.26t^{-3} + 1.49t^{-2} + 1.84t^{-3/2} + 0.16t^{-1} - 0.38t^{-1/2} + 0.72 + 0.67t^{1/2} - 0.18t - 0.22t^{3/2} + 0.22t^2 - 0.07t^3$$

$$f_{w(0.22)} = -0.59t^{-3} + 2.15t^{-2} + 1.83t^{-3/2} - 0.81t^{-1} - 1.02t^{-1/2} + 1.39 + 1.59t^{1/2} - 0.21t - 0.53t^{3/2} - 0.27t^2 - 0.08t^3$$

$$f_{w(0.44)} = -0.92t^{-3} + 2.83t^{-2} + 1.67t^{-3/2} - 1.86t^{-1} - 1.53t^{-1/2} + 2.27 + 2.39t^{1/2} - 0.45t - 0.85t^{3/2} + 0.53t^2 - 0.16t^3$$

royalsocietypublishing.org/journal/rspa *Proc. R. Soc. A* **478**: 20220302

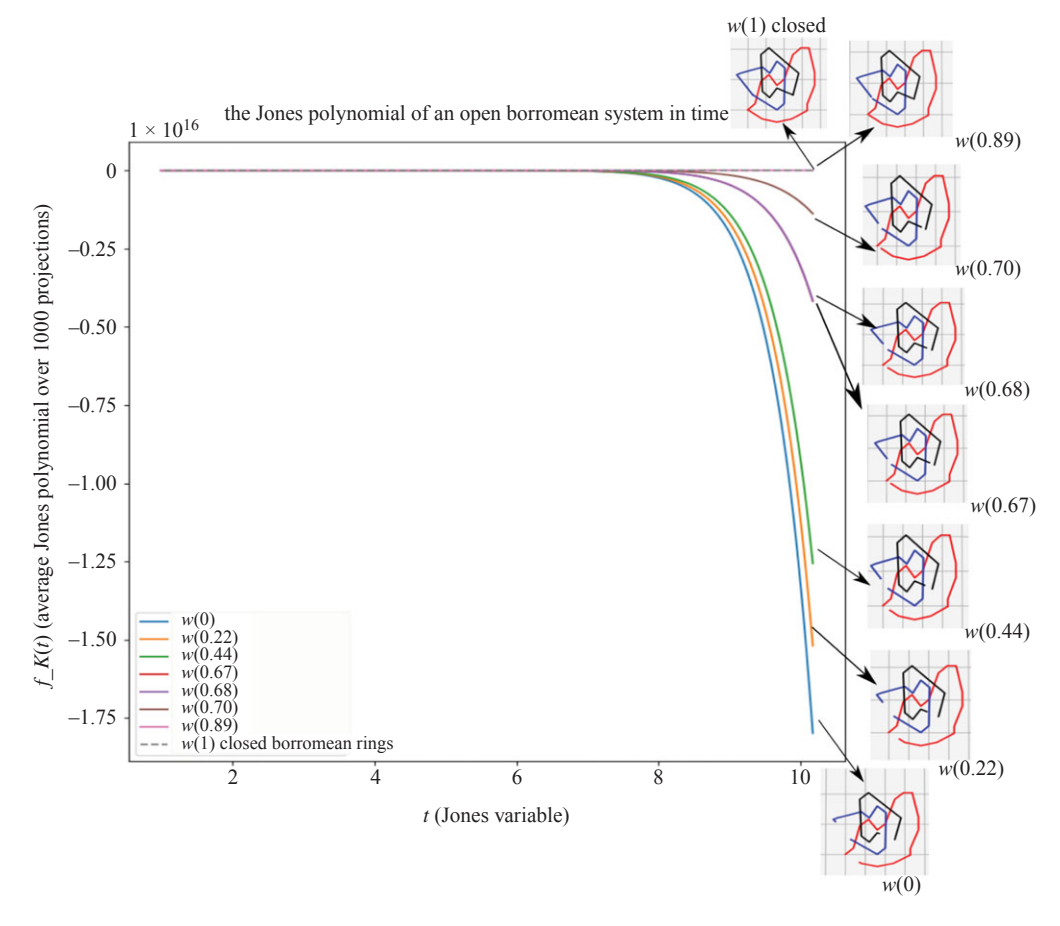


Figure 9. The Jones polynomial of a system of open borromean rings in 3-space as the endpoints move closer in time to ultimately give rise to the closed borromean rings in 3-space. The coefficients of the Jones polynomial are a continuous function of the chain coordinates.

$$\begin{split} f_{w(0.67)} &= -0.98t^{-3} + 2.95t^{-2} + 1.45t^{-3/2} - 2.04t^{-1} - 1.4t^{-1/2} \\ &\quad + 2.60 + 2.22t^{1/2} - 0.68t - 0.78t^{3/2} + 0.86t^2 - 0.27t^3 \\ f_{w(0.68)} &= -0.98t^{-3} + 2.94t^{-2} + 1.43t^{-3/2} - 2.02t^{-1} - 1.39t^{-1/2} \\ &\quad + 2.60 + 2.19t^{1/2} - 0.68t - 0.77t^{3/2} + 0.88t^2 - 0.28t^3 \\ f_{w(0.70)} &= -0.98t^{-3} + 2.96t^{-2} + 1.38t^{-3/2} - 2.04t^{-1} - 1.34t^{-1/2} \\ &\quad + 2.66 + 2.11t^{1/2} - 0.74t - 0.75t^{3/2} + 0.96t^2 - 0.31t^3 \\ f_{w(0.89)} &= -0.99t^{-3} + 2.98t^{-2} + 0.18t^{-3/2} - 2.06t^{-1} - 0.17t^{-1/2} \\ &\quad + 3.86 + 0.35t^{1/2} - 1.9t - 0.15t^{3/2} + 2.74t^2 - 0.9t^3 \\ f_{w(1)} &= -t^{-3} + 3t^{-2} - 2t^{-1} + 4 - 2t + 3t^2 - t^3 \end{split}$$

Note that $f_{w(0)}$ is a new polynomial representing the particular configuration of the open borromean ring in 3-space. This is a polynomial with real coefficients, while $f_{w(1)}$ is the integer polynomial invariant of the borromean ring. We note that, as the endpoints of the open link tend to coincide, the coefficients of the powers of t that compose the borromean ring tend to their corresponding integer values, while the coefficients of the powers of t that are not part of the borromean ring, tend to zero.

5. Conclusion

In this manuscript, we introduced the first measure of topological complexity of collections of open curves in 3-space, based on a novel Jones polynomial. The classical Jones polynomial is a special case of this novel Jones polynomial. For collections of open curves in 3-space, the novel Jones polynomial is a polynomial with real coefficients, which are continuous functions of the curve coordinates and, as the endpoints of the curves tend to coincide, it tends to the integer coefficient, Jones polynomial invariant of the resulting link.

The definition of the Jones polynomial of open curves in 3-space is based on a novel definition of the Jones polynomial of linkoids that we introduced in this manuscript as well. This novel Jones polynomial of linkoids is the only such definition that satisfies the basic property that the polynomial of a link-type linkoid is that of corresponding link. This polynomial thus generalizes the Jones polynomial of knotoids, while maintaining its properties. This new definition of the Jones polynomial of linkoids will enable to properly define other invariants of linkoids as well in the future.

We demonstrated with numerical examples how the novel Jones polynomial of open curves in 3-space can be useful in practice to characterize multi-chain complexity for the first time. This enables the rigorous characterization of multi-chain entanglement in many physical systems obtained either from experiments or simulations, such as polymers and biopolymers, where entanglement is arguably an important factor of mechanics and function, which has been elusive.

Data accessibility. This article has no additional data.

Authors' contributions. K.B.: conceptualization, data curation, formal analysis, investigation, methodology, project administration, resources, software, validation, visualization, writing—original draft, writing—review and editing; E.P.: conceptualization, formal analysis, funding acquisition, investigation, methodology, project administration, resources, software, supervision, validation, writing—review and editing.

Both authors gave final approval for publication and agreed to be held accountable for the work performed therein.

Conflict of interest declaration. We declare we have no competing interests.

Funding. Kasturi Barkataki and Eleni Panagiotou were supported by NSF (grant nos. DMS-1913180 and NSF CAREER 2047587).

Appendix A

Downloaded from https://royalsocietypublishing.org/ on 06 January 2023

In §3a, we introduced the definitions of orbits and segment cycles in the context of linkoid states. In this section, we provide a few supplementary remarks about some interesting properties of these structures. We also prove the result that the number of segment cycles in a state is bounded between 1 and n in proposition A.9. Let L denote a linkoid with n components and n be the set of the endpoints of its components. Note that for any linkoid, there is an associated trivial pairing n and for any state of the linkoid, there exists a pairing combination n.

Remark A.1. (Inverses of pairing combinations and their compositions) For any element $a \in G$, if J(a) = b, then $J^2(a) = J(b) = a$. Therefore, $J^{-1}(a) = J(a)$. Similarly, $\Gamma^{-1}(a) = \Gamma(a)$. We combine these two results to conclude that $(\Gamma \circ J)^{-1} = J^{-1} \circ \Gamma^{-1} = J \circ \Gamma$. Also, $(\Gamma \circ J)^0 = Id_G$, i.e. the identity map on the set G.

Remark A.2. (Orbit of an endpoint is a non-empty set) $\forall a \in G$, $\operatorname{Orb}_J(a) \neq \emptyset$ since, $a = (\Gamma \circ J)^0(a) \in \operatorname{Orb}_J(a)$.

Proposition A.3. *For* $a \in G$, $\Gamma(a) \notin Orb_I(a)$.

Proof. Note that $\operatorname{Orb}_{J}(a)$ is a finite set because the set $|G| = 2n < \infty$. Therefore, $\exists m \in \mathbb{N}$ such that $(\Gamma \circ J)^{m}(a) = a$.

royalsocietypublishing.org/journal/rspa Proc. R. Soc. A **478**: 20220302

Suppose $\Gamma(a) \in \operatorname{Orb}_{J}(a)$. Then, $\exists k < m \in \mathbb{N}$ such that, $(\Gamma \circ J)^{k}(a) = \Gamma(a)$. We know,

$$(\Gamma \circ J)^{m-1}(a) = \alpha$$
 for some $\alpha \neq a$
 $\Longrightarrow J(\Gamma \circ J)^{m-1}(a) = \Gamma(a)$ (A 1)
 $\Longrightarrow J(\Gamma \circ J)^{m-1}(a) = (\Gamma \circ J)^k(a)$

This restricts k to lie between m-1 and m. Note that, k cannot be m-1 since $k \in \mathbb{N}$ being a pairing combination can never map an endpoint to itself. Therefore, there exists no $k \in \mathbb{N}$ that ensures $\Gamma(a) \in \operatorname{Orb}_I(a)$.

Proposition A.4. Let $a, b \in G$ where G is the set of all endpoints of an n component linkoid diagram, L. Let a pairing combination, J be defined on G. If $b \in Orb_{J}(a)$, then $Orb_{J}(b) = Orb_{J}(a)$.

Proof. We have, $b \in \operatorname{Orb}_I(a) \Longrightarrow b = (\Gamma \circ J)^m(a)$, where $m \in \mathbb{Z}$.

Any $x \in \operatorname{Orb}_J(b)$ can be expressed as $x = (\Gamma \circ J)^p(b)$ for some $p \in \mathbb{Z}$. Substituting b, we get $x = (\Gamma \circ J)^p(\Gamma \circ J)^m(a) = (\Gamma \circ J)^{p+m}(a) \Longrightarrow x \in \operatorname{Orb}_J(a)$.

For any $y \in Orb_J(a)$, we can express $y = (\Gamma \circ J)^q(a)$ for some $q \in \mathbb{Z}$. This expression can be manipulated to give $y = (\Gamma \circ J)^{q-m}(\Gamma \circ J)^m(a) = (\Gamma \circ J)^{q-m}(b) \Longrightarrow y \in Orb_J(b)$.

Therefore,
$$Orb_I(b) = Orb_I(a)$$
.

Proposition A.5. For a pairing combination, J, defined on G, we have $\Gamma(\operatorname{Orb}_J(a)) = \operatorname{Orb}_J(\Gamma(a))$, where $a \in G$.

Proof. We prove the proposition by showing element-wise containment. Let,

$$x \in \Gamma(Orb_{J}(a))$$

$$\iff x = \Gamma(\Gamma \circ J)^{m}(a) \quad \text{for some } m \in \mathbb{Z}$$

$$\iff x = \Gamma(\Gamma \circ J)^{m}\Gamma(\Gamma(a))$$

$$\iff x = \Gamma(\Gamma(J \circ \Gamma)^{m})(\Gamma(a))$$

$$\iff x = (J \circ \Gamma)^{m}(\Gamma(a))$$

$$\iff x = (\Gamma \circ J)^{-m}(\Gamma(a))$$

$$\iff x \in Orb_{J}(\Gamma(a)) \tag{A 2}$$

Therefore, $\Gamma(\operatorname{Orb}_{I}(a)) = \operatorname{Orb}_{I}(\Gamma(a))$.

Proposition A.6. Let $a, b \in G$. If $b \in Seg(a)$, then Seg(b) = Seg(a) and they will correspond to the same decorated circle.

```
Proof. We have, b \in \operatorname{Seg}(a) \Longrightarrow \operatorname{either} b \in \operatorname{Orb}_J(a) or b \in \operatorname{Orb}_J(\Gamma(a)).

If b \in \operatorname{Orb}_J(a), then we know from proposition A.4 that \operatorname{Orb}_J(b) = \operatorname{Orb}_J(a)

\Longrightarrow \Gamma(\operatorname{Orb}_J(b)) = \Gamma(\operatorname{Orb}_J(a)) \Longrightarrow \operatorname{Orb}_J(\Gamma(b)) = \operatorname{Orb}_J(\Gamma(a)).

Therefore, \operatorname{Seg}(b) = \operatorname{Seg}(a).

If b \in \operatorname{Orb}_J(\Gamma(a)) = \Gamma(\operatorname{Orb}_J(a)), then \Gamma(b) \in \operatorname{Orb}_J(a). By proposition A.4,

\operatorname{Orb}_J(\Gamma(b)) = \operatorname{Orb}_J(a) \Longrightarrow \Gamma(\operatorname{Orb}_J(\Gamma(b))) = \Gamma(\operatorname{Orb}_J(a)) \Longrightarrow \operatorname{Orb}_J(b) = \operatorname{Orb}_J(\Gamma(a)).

Therefore, \operatorname{Seg}(b) = \operatorname{Seg}(\Gamma(b)) = \operatorname{Seg}(a). ▮
```

In the following example, we construct the segment cycle that results due to the state in figure 10.

Example A.7. Consider the linkoid diagram and the particular state (say S), as shown in figure 10. Here, the set G of all endpoints is $\{1,2,3,4,5,6\}$. The pairwise connections among these endpoints in the state S can be represented by the bijective map, $J_S: G \to G$, which can be represented as a permutation $J_S = (1 \ 3)(2 \ 6)(4 \ 5)$. Using this map, the segment cycle of the endpoint labelled 1 turns out to be the entire set G. Note that this is the only distinct segment

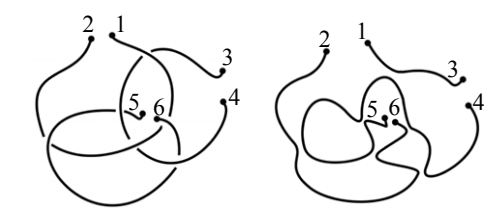


Figure 10. (Left) A linkoid diagram with three components, $I_{(1,2)}$, $I_{(3,4)}$ and $I_{(5,6)}$. (Right) One of the 64 possible states in the state sum expansion of the diagram. Clearly, this state is crossingless and contains three disjoint segments, namely (1, 3), (2, 6) and (4, 5). Note that even though the number of long segments is the same as the number of components of the original linkoid, there has been a rearrangement in the pairing of endpoints per segment.

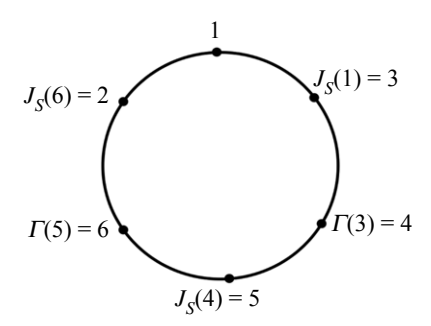


Figure 11. Representation of the segment cycle in terms of a decorated circle for the state *S* in figure 10 with $J_S = (1 \ 3)(2 \ 6)(4 \ 5)$.

Downloaded from https://royalsocietypublishing.org/ on 06 January 2023

cycle that results from the action of J_S on G and it can be represented as the decorated circle shown in figure 11.

Recall that $\Gamma \circ J \in S_{2n}$. Thus, $\langle \Gamma \circ J \rangle$ is a cyclic subgroup of S_{2n} . Also, $\langle \Gamma \rangle$ is a cyclic subgroup of S_{2n} . It follows that their direct product, $\mathcal{G} = \langle \Gamma \circ J \rangle \times \langle \Gamma \rangle$, is a subgroup of S_{2n} . The following remark uses these facts to provide alternative definitions for orbits and segment cycles in terms of equivalence classes under group actions.

Remark A.8. (Orbits and segment cycles as equivalence classes) The orbit of an endpoint can be also defined as the equivalence class of the endpoint (as an element of G) under the equivalence relation $\mathcal{R}_{\langle \Gamma \circ J \rangle}$ on the set G. Similarly, the segment cycle of an element $a \in G$ can be defined as the orbit of G under the action of G as shown below:

$$Seg(a) = Orb_{\mathcal{G}}(a) := \{ y \in G | \exists (g, h) \in \mathcal{G} | y = (g, h) \star a \}, \tag{A 3}$$

where \star means the group action such that $(g,h) \star a = g(h(a))$, the image of a with respect to the composition function $g \circ h$. The quotient set $G/\mathcal{R}_{\mathcal{G}}$, where $\mathcal{R}_{\mathcal{G}}$ is the equivalence relation induced by \mathcal{G} , gives the set of all segment cycles. The cardinality of this set gives the total number of distinct segment cycles due to the pairing combination J.

Proof. For a pairing combination J_S corresonding to a state S of a linkoid diagram, remark A.8 implies:

$$\mathcal{G} = \langle \Gamma \circ J_S \rangle \times \langle \Gamma \rangle
\supseteq \langle id \rangle \times \langle \Gamma \rangle
= \{id\} \times \{id, \Gamma\}
= \{(id, id), (id, \Gamma)\} := \mathcal{H}.$$
(A4)

Therefore, the equivalence relation $\mathcal{R}_{\mathcal{G}}$ on G implies:

$$\operatorname{Orb}_{\mathcal{G}}(a) \supseteq \operatorname{Orb}_{\mathcal{H}}(a) \\
= \left\{ (id, id) \star a, (id, \Gamma) \star a \right\} \\
= \left\{ id(id(a)), id(\Gamma(a)) \right\} \\
= \left\{ id(id(a)), id(\Gamma(a)) \right\} \\
= \left\{ a, \Gamma(a) \right\} \quad \text{for any element } a \in G. \tag{A 5}$$

Thus, the minimum cardinality of the segment cycle of a point $a \in G$ is equal to 2. When J_S is the trivial pairing combination Γ , the set G is equipartitioned into n classes (segment cycles). Therefore, the maximum number of distinct segment cycles that can occur for a linkoid state is n.

Equation (A 5) also implies that $\operatorname{Orb}_{\mathcal{G}}(a) \neq \emptyset$ for all pairing combination J_S . Therefore, the total number of segment cycles corresponding to a state S can never be zero. Note that in the cases where $\operatorname{Orb}_{\mathcal{G}}(a) = G$, the total number of segment cycles corresponding to the state is equal to 1.

Thus, we have the bound: $1 \le |S|_{\text{cyc}} \le n$.

References

Downloaded from https://royalsocietypublishing.org/ on 06 January 2023

- 1. Arsuaga J, Vazquez M, McGuirk P, Trigueros S, Sumners DW, Roca J. 2005 DNA knots reveal a chiral organization of DNA in phage capsids. *Proc. Natl Acad. Sci. USA* **102**, 9165–9169. (doi:10.1073/pnas.0409323102)
- 2. Edwards SF. 1967 Statistical mechanics with topological constraints: I. *Proc. Phys. Soc.* 91, 513–9. (doi:10.1088/0370-1328/91/3/301)
- 3. Liu Y, O'Keeffe M, Treacy M, Yaghi O. 2018 The geometry of periodic knots, polycatenanes and weaving from a chemical perspective: a library for reticular chemistry. *Chem. Soc. Rev.* 47, 4642–4664. (doi:10.1039/C7CS00695K)
- Panagiotou E, Millett KC, Atzberger PJ. 2019 Topological methods for polymeric materials: characterizing the relationship between polymer entanglement and viscoelasticity. *Polymers* 11, 11030437. (doi:10.3390/polym11030437)
- 5. Qin J, Milner ST. 2011 Counting polymer knots to find the entanglement length. *Soft Matter* 7, 10676–93. (doi:10.1039/c1sm05972f)
- Ricca R. 2008 Topology bounds energy of knots and links. Proc. R. Soc. A 464, 293–300. (doi:10.1098/rspa.2007.0174)
- Sulkowska JI, Rawdon EJ, Millett KC, Onuchic JN, Stasiak A. 2012 Conservation of complex knotting and slipknotting in patterns in proteins. *Proc. Natl Acad. Sci. USA* 109, E1715. (doi:10.1073/pnas.1205918109)
- 8. Taylor JB. 1974 Relaxation of toroidal plasma and generation of reverse magnetic fields. *Phys. Rev. Lett.* **33**, 1139. (doi:10.1103/PhysRevLett.33.1139)
- 9. De Gennes PG. 1974 The physics of liquid crystals. Oxford, UK: Clarendon Press.
- Edwards SF. 1968 Statistical mechanics with topological constraints: II. *J. Phys. A: Gen. Phys.* 1, 15–28. (doi:10.1088/0305-4470/1/1/303)
- 11. Gauss K. F. 1877 Zur mathematischen Theorie der electrodynamischen Wirkungen, 1833, Werke, Königlichen Gesellschaft der Wissinchaften zu Gottingen 5, 602–629.
- Werke, Königlichen Gesellschaft der Wissinchaften zu Gottingen 5, 602–629.
 Panagiotou E. 2015 The linking number in systems with periodic boundary conditions. *J. Comput. Phys.* 300, 533–573. (doi:10.1016/j.jcp.2015.07.058)

- 13. Panagiotou E, Kröger M. 2014 Pulling-force-induced elongation and alignment effects on entanglement and knotting characteristics of linear polymers in a melt. *Phys. Rev. E* **90**, 042602. (doi:10.1103/PhysRevE.90.042602)
- 14. Panagiotou E, Kröger M, Millett KC. 2013 Writhe and mutual entanglement combine to give the entanglement length. *Phys. Rev. E* **88**, 062604. (doi:10.1103/PhysRevE.88.062604)
- 15. Panagiotou E, Tzoumanekas C, Lambropoulou S, Millett KC, Theodorou DN. 2011 A study of the entanglement in systems with periodic boundary conditions. *Progr. Theor. Phys. Suppl.* **191**, 172–181. (doi:10.1143/PTPS.191.172)
- Panagiotou E, Kauffman L. 2020 Knot polynomials of open and closed curves. *Proc. R. Soc. A* 476, 20200124. (doi:10.1098/rspa.2020.0124)
- 17. Panagiotou E, Kauffman L. 2021 Vassiliev measures of complexity for open and closed curves in 3-space. *Proc. R. Soc. A* 477, 20210440. (doi:10.1098/rspa.2021.0440)
- 18. Herschberg T, Carrillo J-MY, Sumpter BG, Panagiotou E, Kumar R. 2021 Topological effects near order–disorder transitions in symmetric diblock copolymer melts. *Macromolecules* **54**, 7492–7499. (doi:10.1021/acs.macromol.1c00780)
- 19. Smith P, Panagiotou E. 2022 The second vassiliev measure of uniform random walks and polygons in confined space. *J. Phys. A: Math. Theor.* **55**, 095601. (doi:10.1088/1751-8121/ac4abf)
- 20. Wang J, Panagiotou E. 2022 The protein folding rate and the geometry and topology of the native state. *Sci. Rep.* **12**, 6384. (doi:10.1038/s41598-022-09924-0)
- 21. Turaev V. 2012 Knotoids. Osaka, J. Math. 49, 195-223.
- 22. Gügümcu N, Kauffman LH. 2017 New invariants of knotoids. Eur. J. Comb. 65, 186-229.
- 23. Gügümcu N, Kauffman LH. 2019 Parity in knotoids, pp. 1–19. (http://arxiv.org/abs/1905. 04089)
- 24. Gügümcu N, Lambropoulou S. 2017 Knotoids, braidoids and applications. Symmetry 9, 315.
- 25. Manouras M, Lambropoulou S, Kauffman LH. 2021 Finite type invariants for knotoids. *Eur. J. Comb.* **98**, 103402. (doi:10.1016/j.ejc.2021.103402)
- Gabrovšek B, Gügümcü N. 2022 Invariants of multi-linkoids. (http://arxiv.org/abs/2204. 11234)